


Gate-Efficient Simulation of Molecular Eigenstates on a Quantum Computer

M. Ganzhorn,^{1,*} D.J. Egger,¹ P. Barkoutsos,¹ P. Ollitrault,¹ G. Salis,¹ N. Moll,¹ M. Roth,^{2,3} A. Fuhrer,¹ P. Mueller,¹ S. Woerner,¹ I. Tavernelli,¹ and S. Filipp¹

¹IBM Research Zurich, Säumerstrasse 4, 8803 Rüschlikon, Switzerland

²JARA Institute for Quantum Information (PGI-11), Forschungszentrum Jülich, 52428 Jülich, Germany

³Institute for Quantum Information, RWTH Aachen University, 52056 Aachen, Germany

 (Received 18 October 2018; revised manuscript received 5 March 2019; published 30 April 2019)

A key requirement to perform simulations of large quantum systems on near-term quantum hardware is the design of quantum algorithms with a short circuit depth that finish within the available coherence time. A way to stay within the limits of coherence is to reduce the number of gates by implementing a gate set that matches the requirements of the specific algorithm of interest directly in the hardware. Here, we show that exchange-type gates are a promising choice for simulating molecular eigenstates on near-term quantum devices since these gates preserve the number of excitations in the system. We report on the experimental implementation of a variational algorithm on a superconducting qubit platform to compute the eigenstate energies of molecular hydrogen. We utilize a parametrically driven tunable coupler to realize exchange-type gates that are configurable in amplitude and phase on two fixed-frequency superconducting qubits. With gate fidelities around 95%, we are able to compute the eigenstates to within an accuracy of 50 mHa (milliHartree) on average, a limit set by the coherence time of the tunable coupler.

DOI: [10.1103/PhysRevApplied.11.044092](https://doi.org/10.1103/PhysRevApplied.11.044092)

I. INTRODUCTION

The simulation of the electronic structure of molecular and condensed-matter systems is a challenging computational task, as the cost of resources increases exponentially with the number of electrons when accurate solutions are required. With the tremendous improvements in the control of complex quantum systems, this bottleneck may be overcome by the use of quantum-computing hardware [1]. Various algorithms for quantum simulation have been designed to that end, including adiabatic and quantum phase estimation algorithms [2,3]. With these algorithms, the challenges for practical applications lie in the efficient mapping of the electronic Hamiltonian onto the quantum computer and in the required number of quantum gates, respectively, which remains prohibitive on current and near-term quantum hardware [4] without quantum error-correction schemes [5]. On the other hand, variational quantum eigensolver (VQE) methods [6,7] can produce accurate results with a small number of gates [8], using algorithms with a low circuit depth [9], and do not require a direct mapping of the electronic Hamiltonian onto the hardware. Moreover, such algorithms are inherently robust against certain errors [8,10,11] and are therefore considered as ideal candidates for first practical implementations on noisy intermediate-scale quantum hardware.

Recently, the molecular ground-state energy of hydrogen and helium have been computed via VQE in proof-of-concept experiments using nuclear-magnetic-resonance (NMR) quantum simulators [12–14], photonic architectures [6], or nitrogen-vacancy centers in diamond [15]. Although very accurate energy estimates are obtained, quantum simulation of larger systems remains an intractable problem on these platforms because of the difficulties arising in scaling them up to more than a few qubits. For this reason, trapped ions [16–19] and superconducting qubits [20–22] have become promising candidates to carry out VQE-based quantum simulations, particularly for quantum-chemistry applications. For instance, the ground-state energies of molecules such as H₂ [23–25], LiH, and BeH₂ [24], as well as the energy spectrum of the four eigenstates of H₂ [25], have been measured on general-purpose superconducting qubit platforms. In these experiments, a heuristic approach based on gates naturally available in the hardware, such as C-phase, CNOT, or bSWAP, is employed. However, the computation of larger molecules with more orbitals in the active computational space becomes impractical with this method. Without further constraints, the dimension of the Hilbert space accessed via the parameterized gate sequences grows exponentially with the number of required qubits N . The probability of reaching the desired ground state decreases accordingly. It is, thus, important to use a set of entangling gates that matches the specifics of the problem [8]. For quantum-chemistry calculation, each qubit typically

*anz@zurich.ibm.com

represents the population of an electronic orbital [26,27]. Since the number of electrons n_e is constant for a given molecular system or chemical reaction, the number of qubit excitations is also constant. Qubit gates that preserve the number of excitations on the qubit processor are, therefore, better suited than other two-qubit gates to compute molecular eigenstates [8,28]. In fact, the use of only excitation-preserving gates constrains the accessible state space to a subspace of the full 2^N -dimensional Hilbert space: only the (N_{n_e}) -dimensional manifold with n_e electrons is explored in VQE, which simplifies the construction of a reduced molecular Hamiltonian [7] and the expansion of the trial wave function [8].

In this paper, we show an efficient and scalable approach to computing the energy spectrum of molecules using excitation-preserving exchange-type two-qubit gates. We demonstrate in simulation that the circuit depth required to achieve chemical accuracy in VQE algorithms can be significantly reduced by using exchange-type gates, which would allow the simulation of larger quantum systems on near-term quantum hardware. We implement such an exchange-type gate-based VQE algorithm on a hardware platform consisting of two fixed-frequency superconducting qubits coupled via a tunable coupler [29,30] and determine the ground-state energy of molecular hydrogen. Finally, we efficiently derive the excited states of molecular hydrogen from the measured ground state using the equation-of-motion (EOM) approach [31], which complements the quantum subspace expansion (QSE) in Refs. [25,32].

II. GATE-EFFICIENT QUANTUM CIRCUITS

In quantum chemistry, the molecular Hamiltonian is represented in second quantization [7,11] as a sum of one- and two-body terms and then mapped to the qubit space using a fermion-to-qubit transformation, such as the Jordan-Wigner [26] or the parity-mapping transformation [33]. Suitable trial states for VQE can be computed with a unitary-coupled-cluster (UCC) ansatz [34], which is, however, costly in terms of quantum gates [7,8]. Alternatively, trial states are generated heuristically by a parametrized sequence of gates directly available in hardware [8]. In the original formulation [24], the heuristic trial wave function was generated in the full Fock space, thus including states with all possible numbers of electrons. With each qubit being mapped to the population of an electronic orbital, this corresponds to a Hilbert space spanned by the 2^N basis states $\{i_1, i_2, \dots, i_N\}$, with $i_k = 0, 1$. However, if the solution of interest lies in the sector of the Hilbert space with a well-defined number of electrons n_e , i.e., when $\sum_k i_k = n_e$, it is advantageous to use gates that conserve the total number of excitations over the entire qubit register for the trial-state preparation.

The simplest method is to prepare the initial state with n_e qubit excitations, e.g., $|1_1, 1_2, \dots, 1_{n_e}, 0, \dots, 0\rangle$, and apply only gates ($\hat{\sigma}^+ + \hat{\sigma}^- + h.c.$) that exchange excitations between qubits by creating ($\hat{\sigma}^+$) and annihilating ($\hat{\sigma}^-$) excitations at the same time. The size of the restricted subspace is then given by $(N_{n_e}) \leq 2^N$. Close to half-filling with $n_e \approx N/2$, the advantage is small, since $(N_{n_e}) \approx 2^{N/2}$. For many molecules, however, the number of electrons is typically $n_e \approx N/10$ [35] and the size of the restricted subspace $(N_{n_e}) \approx (N/n_e)^{n_e}$ is significantly smaller than that of the full Hilbert space. We note that the restriction of the search space to a given number of electrons prevents the VQE from getting trapped in local minima with an unphysical number of electrons, which is beneficial in particular for multielectron systems.

In a VQE simulation, the size of the explored subspace is directly connected to the circuit depth required to reach a certain accuracy. Assuming error-free gates and using the minimal basis set of atomic orbitals typically used in quantum chemistry [36], we estimate the circuit depth required to achieve chemical accuracy in a VQE simulation of the molecules H_2 , LiH, BeH₂, and H₂O (see Fig. 1) [37]. Heuristic non-excitation-conserving circuits, based, e.g., on CNOT gates [24,38], can in principle achieve chemical accuracy for these molecules. However, the required circuit depth becomes prohibitively large for molecules bigger than H_2 as the circuit run time exceeds the best relaxation times, $T_1 \sim 100 \mu s$, currently available in superconducting hardware. On the other hand, circuits based on excitation-conserving exchange-type gates require a much shorter circuit depth and achieve chemical accuracy for all studied cases within the T_1 limit without further amendments (Fig. 1). Clearly, the desired excitation-preserving two-qubit gate could be decomposed into the available universal gate set [39,40], e.g., by using CNOT gates. But this comes at the expense of an at least tenfold increase in circuit depth (Fig. 1), which can be avoided by using application-specific hardware and gates. We note that additional reduction schemes can be used to minimize the number of qubits, as demonstrated in Ref. [24] for H_2 , LiH, BeH₂ and as discussed in the following for the proof-of-principle determination of the eigenspectrum of H_2 .

III. EXCHANGE-TYPE GATES IN A TUNABLE-COUPLER ARCHITECTURE

An exchange-type gate primitive can naturally be realized in a tunable-coupler architecture (Fig. 2) [29,30,41]. The device consists of two fixed-frequency transmon qubits, $Q1$ and $Q2$, linked via a tunable coupler (TC), i.e., a frequency-tunable transmon [37]. An exchange-type coupling between the computational qubits $Q1$ and $Q2$ is achieved by parametric modulation of the TC frequency

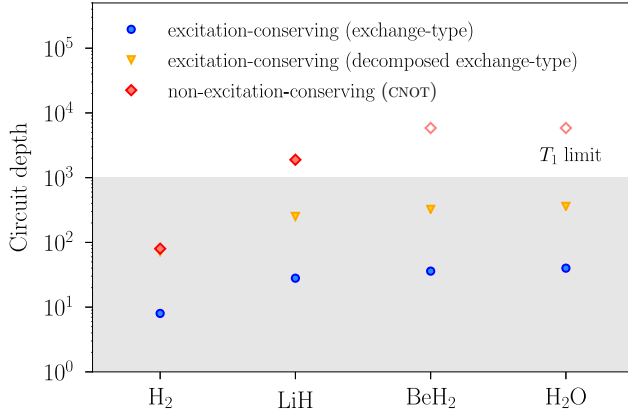


FIG. 1. The circuit depth required to achieve chemical accuracy for the ground-state energy with a VQE algorithm for the H_2 , LiH , BeH_2 , and H_2O molecules. Non-excitation-conserving circuits based on CNOT gates (red squares) are compared to excitation-conserving circuits based on exchange-type gates (blue circles) and a decomposition thereof into CNOT gates (yellow triangles). In some cases, only a lower boundary to the circuit depth can be estimated (empty symbols). Bounded by the T_1 time in the currently available hardware, only circuits within the gray region can be implemented in practice without error mitigation or reduction schemes (see text).

$\omega_c(t) = \omega_c^0 \sqrt{|\cos(\pi \Phi(t)/\Phi_0)|}$ [29,30]. Threading a magnetic flux $\Phi(t) = \Phi_{\text{DC}} + \delta \cos(\omega_\phi t + \varphi_\phi)$ with $\omega_\phi = \omega_1 - \omega_2$ through the SQUID loop of the TC implements the effective Hamiltonian [30]

$$\hat{H}_{\text{eff}} = -\frac{\Omega_{\text{eff}}}{4} [\cos \varphi (XX + YY) - \sin \varphi (YX - XY)], \quad (1)$$

with the set of Pauli operators $\{X, Y, Z\} \equiv \{\hat{\sigma}_x, \hat{\sigma}_y, \hat{\sigma}_z\}$. It describes an exchange-type interaction between $|10\rangle$ and $|01\rangle$ at a rate $\Omega_{\text{eff}}(\Phi_{\text{DC}}, \delta)$ [Fig. 2(c)]. In the following, $\Phi_{\text{DC}} = 0.195\Phi_0$ if not stated otherwise. The resulting two-qubit gate operation is described by the unitary operator

$$\hat{U}_{\text{EX}}(\theta, \varphi) = \begin{pmatrix} 1 & 0 & 0 & 0 \\ 0 & \cos \theta/2 & ie^{i\varphi} \sin \theta/2 & 0 \\ 0 & ie^{-i\varphi} \sin \theta/2 & \cos \theta/2 & 0 \\ 0 & 0 & 0 & 1 \end{pmatrix}. \quad (2)$$

Here, $\theta = \Omega_{\text{eff}}\tau = \pi\tau/\tau_\pi$ is controlled by the length τ of the tunable-coupler drive pulse and $\tau_\pi = 170$ ns is the length of an iSWAP gate, which completely transfers an excitation from one qubit to the other. The phase $\varphi = \varphi_\phi$ is controlled by the phase φ_ϕ of the tunable-coupler drive.

To benchmark the efficiency of the exchange-type gate primitive, we perform quantum-process tomography (QPT) of \hat{U}_{EX} as a function of φ for a fixed $\theta = \pi$. The overlap of the measured process matrix $\chi_{\text{meas}}(\varphi)$ with an

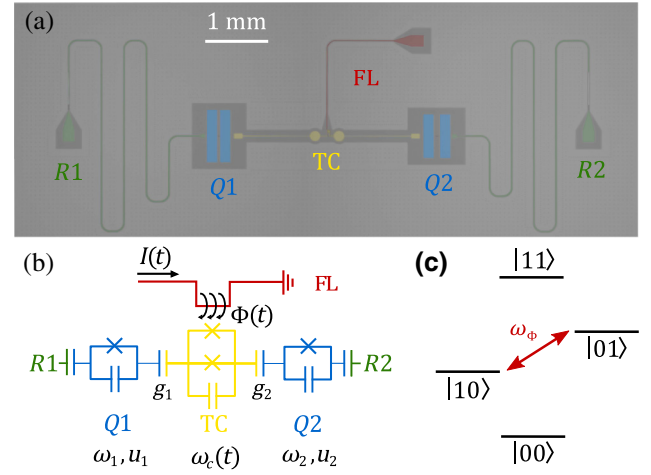


FIG. 2. An (a) optical micrograph and (b) the circuit scheme of the device consisting of two fixed-frequency transmons ($Q1, Q2$) capacitively coupled to a flux-tunable transmon acting as tunable coupler (TC). The tunable coupler is controlled by a flux line (FL) providing a current $I(t)$ and a consequent flux $\Phi(t) = \Phi_{\text{DC}} + \delta \cos(\omega_\phi t + \varphi_\phi)$ threading the superconducting quantum-interference device (SQUID) loop of the coupler. Each of the fixed-frequency qubits is coupled to an individual readout resonator (R1, R2). (c) The level diagram of the device. Here, $|n_1 n_2\rangle$ denotes the state of the combined system with the qubit excitation number $n_{1,2}$. Modulation of the magnetic flux $\Phi(t)$ at the difference frequency $\omega_\phi = \omega_1 - \omega_2$ of the qubits drives the transition between $|10\rangle$ and $|01\rangle$.

ideal process matrix χ_{ideal} yields the gate fidelity $\mathcal{F} = \text{Tr}[\chi_{\text{meas}}(\varphi)\chi_{\text{ideal}}]$. If the measured process matrices are compared with the ideal process matrix of a $\hat{U}_{\text{EX}}(\pi, \varphi)$ operation, the gate fidelity is constant over φ , with an average of $\mathcal{F} = 94.2 \pm 1.5\%$ [Fig. 3(a)]. However, if the measured process matrices are compared with the ideal process matrix of $\hat{U}_{\text{EX}}(\pi, 0)$, equivalent to an iSWAP-gate operation, the gate fidelity is phase dependent. A fit with the analytic expression

$$\mathcal{F}_{\text{ana}} = \mathcal{F}_0 |e^{-2i(\varphi-\varphi_0)} (1 + e^{i(\varphi-\varphi_0)})^4| \quad (3)$$

yields a maximum gate fidelity of $\mathcal{F}_0 = 93.2 \pm 0.5\%$, achieved for $\varphi_0 = 3 \pm 5$ mrad [Fig. 3(a)]. Similarly, a comparison with the ideal process matrix of $\hat{U}_{\text{EX}}(\pi, \pi/2)$ and $\hat{U}_{\text{EX}}(\pi, \pi)$ yields maximum gate fidelities at $\varphi_0 = 1.574 \pm 0.007$ rad and $\varphi_0 = 3.155 \pm 0.006$ rad, respectively. It should be noted that the gate-fidelity estimation via QPT is subject to state preparation and measurement (SPAM) errors. Other techniques, such as randomized benchmarking, are robust against such SPAM errors, but are mostly limited to gates from the Clifford group. For an iSWAP as a two-qubit gate primitive, we find an error per gate of 3.7% via randomized benchmarking [37].

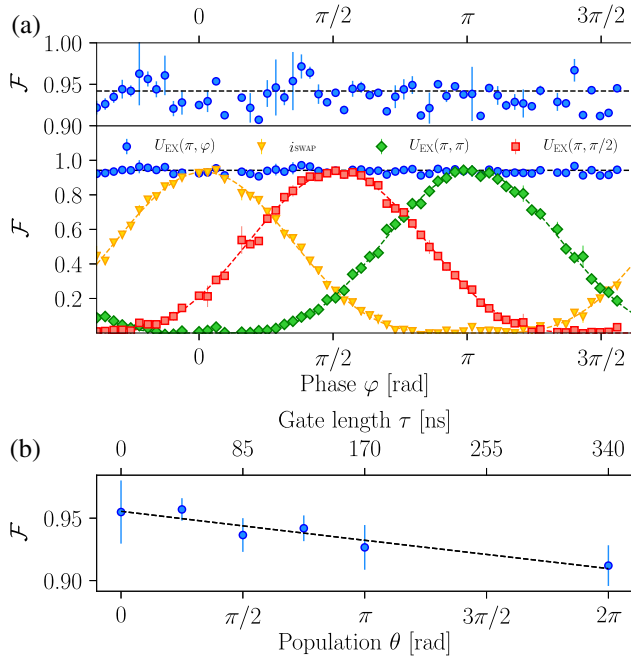


FIG. 3. Quantum-process tomography of the chemistry gate $\hat{U}_{\text{EX}}(\theta, \varphi)$. (a) The gate fidelities \mathcal{F} as a function of φ for $\theta = \pi$. The bottom panel shows the gate fidelities calculated from the overlap of the measured process matrices $\chi_{\text{meas}}(\varphi)$ with the ideal process matrix χ_{ideal} of a $\hat{U}_{\text{EX}}(\pi, \varphi)$ (blue dots), *i*SWAP (orange triangles), $\hat{U}_{\text{EX}}(\pi, \pi/2)$ (red squares), and $\hat{U}_{\text{EX}}(\pi, \pi)$ (green diamonds) gate operation. The top panel shows the gate fidelities with respect to $\hat{U}_{\text{EX}}(\pi, \varphi)$. The black dashed lines depict the average gate fidelity for $\hat{U}_{\text{EX}}(\pi, \varphi)$ (see text). The colored dashed lines are a fit to Eq. (3). (b) The gate fidelities \mathcal{F} as a function of θ , where the phase φ_{opt} is tuned to maximize the QPT fidelity. The dashed line is a fit with an exponential decay function, with a decay time of $6.7 \mu\text{s}$.

Furthermore, we perform QPT of \hat{U}_{EX} as a function of θ , i.e., for different lengths τ of the drive pulse on the tunable coupler. Comparison of the measured process matrices with the ideal process matrix of $\hat{U}_{\text{EX}}(\theta, \varphi_{\text{opt}})$ yields gate fidelities ranging from $\mathcal{F} = 96 \pm 2.5\%$ (for small θ) to $\mathcal{F} = 91 \pm 1.5\%$ (for large θ) [Fig. 3(b)]. Here, the phase φ_{opt} is calibrated to maximize fidelity. The observed decrease of gate fidelity with increasing θ , i.e., a longer pulse length τ , can be fitted to an exponential function with a decay time of $6.7 \mu\text{s}$, close to the measured relaxation time $T_1 = 6.3 \mu\text{s}$ of the TC.

IV. COMPUTATION OF MOLECULAR ENERGY SPECTRA

To demonstrate the usefulness of this gate, we now compute the ground state and the three excited states of molecular hydrogen. Using a parity-mapping transformation [33], we map the fermionic second-quantized Hamiltonian

of molecular hydrogen to the two-qubit Hamiltonian:

$$\hat{H}_{\text{H}_2} = \alpha_0 II + \alpha_1 ZI + \alpha_2 IZ + \alpha_3 ZZ + \alpha_4 XX, \quad (4)$$

where the α_i denote prefactors that are classically computed as a function of the bond length of the molecule in the STO-3G basis [42] using PYQUANTE [37,43].

To compute the ground state at a given bond length, we use a VQE algorithm as described in Ref. [24]. In our case, the respective trial states are of the form $|\psi(\theta, \varphi)\rangle = a(\theta, \varphi)|01\rangle + b(\theta, \varphi)|10\rangle$ and can be realized in a single step with the exchange-type gate primitive $\hat{U}_{\text{EX}}(\theta, \varphi)$. A simultaneous perturbation stochastic approximation (SPSA) algorithm [44] then searches for a state $|\psi(\theta_{\text{opt}})\rangle = |\psi(\theta_{\text{opt}}, \varphi_{\text{opt}})\rangle$ that minimizes the energy of the molecule $E(\theta_{\text{opt}}, \varphi_{\text{opt}}) = \langle \psi(\theta_{\text{opt}}, \varphi_{\text{opt}}) | \hat{H}_{\text{H}_2} | \psi(\theta_{\text{opt}}, \varphi_{\text{opt}}) \rangle$ for a given bond length [37]. By changing the parameters α_i in Eq. (4) and running the VQE again for the modified Hamiltonian, we compute the ground-state energy of molecular hydrogen as a function of the bond length (Fig. 4).

Furthermore, we compute the excited states of molecular hydrogen following the EOM approach [37]. Using a variational method, we obtain a pseudoeigenvalue system of equations that describes the excitations of the system. The matrix elements of this pseudoeigenvalue system correspond to the expectation values of a modified Hamiltonian with the ground state. For each bond length, we measure these matrix elements using the ground state $|\psi(\theta_{\text{opt}}, \varphi_{\text{opt}})\rangle$ computed previously with VQE and solve the pseudoeigenvalue system classically. The solution of this eigenvalue problem then yields the excited-state energies. For each bond length, we perform five runs of the experiment and plot the minimum value for the ground-state energy and the median value for all excited-state energies [symbols in Fig. 4(a)]. A comparison of this experimental solution with the exact solution from a diagonalization of the Hamiltonian \hat{H}_{H_2} yields the accuracy ΔE [symbols in Fig. 4(b)].

For both ground and excited states, ΔE decreases with the bond length while staying above chemical accuracy (defined here by 6.5 mHa , as in Ref. [8]). In order to understand this behavior, we study the influence of decoherence effects on the accuracy. Using the decoherence rates and solving a Lindblad-type master equation via Qutip [37,45], we obtain ground and excited-state energies that now deviate from the exact solution due to decoherence effects [dashed lines in Figs. 4(a) and 4(b)]. The numerical simulations are in good agreement with the experimental data, indicating that decoherence has a strong influence on the measured accuracy in our experiment. In particular, the short coherence time $T_{2,\text{TC}}^* = 20 \text{ ns}$ of the tunable coupler in the present hardware is identified as the main cause of inaccuracy. Our simulations indicate that tunable couplers with coherence times of $T_{2,\text{TC}}^* > 500 \text{ ns}$ would enable us to reach chemical accuracy and gate fidelities of $\mathcal{F}_{\text{EX}} >$

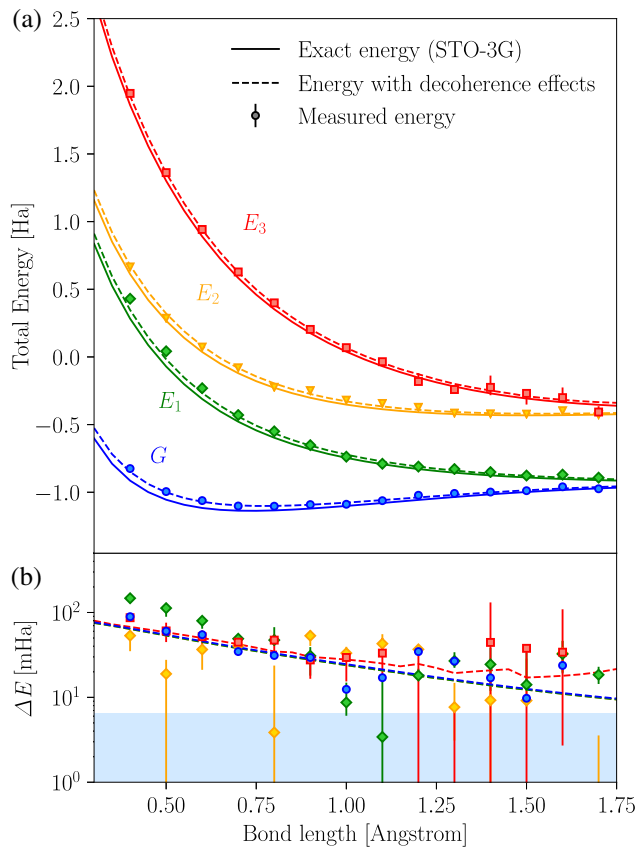


FIG. 4. The experimental VQE solution for the ground state and the EOM solution for the excited states of molecular hydrogen using a tunable-couple architecture. (a) The ground (G) and excited-state (E_1 , E_2 , E_3) energies as a function of the bond length. The symbols depict the experimental VQE solution, the solid lines represent the exact solution from the diagonalization of \hat{H}_{H_2} , and the dashed line represent the solution including decoherence effects. (b) The accuracy for the ground and excited-state energies as a function of the bond length. The symbols correspond to the accuracy of the measured ground and excited-state energies determined with respect to the exact solution, while the dashed lines correspond to the expected accuracy including decoherence effects (see text). The depicted ground-(excited-)state energy is the minimum (median) value from a set of five measurements. The error bars depict the range between the first and third quantile (excited states only). The blue shaded area represents the region of chemical accuracy from 0 to 6.5 mHa.

98.9% for an exchange-type gate in the present architecture, which exhibits a ZZ cross talk between qubits of $\zeta = (\omega_{|11\rangle} - \omega_{|10\rangle} - \omega_{|01\rangle} + \omega_{|00\rangle})/2\pi = -144$ kHz [37]. We note that errors in the optimization and measurement of the ground state $|\psi(\theta_{\text{opt}}, \varphi_{\text{opt}})\rangle$ can induce additional errors in the excited-state energies. For comparison, we evaluate the ground and excited-state energies using the QSE method, described in Refs. [25,32]. Due to the linear response expansion in the qubit space, additional spurious states appear in the molecular spectrum and a larger spread

in the measured accuracies is observed for the QSE method [37]. In contrast, no spurious states appear in the EOM calculations and the accuracy spread is reduced. A detailed analysis of the different errors affecting the excited-state calculation is beyond the scope of this work and will be discussed elsewhere [46].

Furthermore, we evaluate the scalability of our computational methods to larger molecular systems. Using the Qiskit aqua package [47], we estimate the number of Pauli strings $\langle \hat{O}_1 \cdots \hat{O}_N \rangle$ (where $\hat{O} = \{I, X, Y, Z\}$ and N is the number of qubits) required to calculate the ground and excited-state energies to be $\mathcal{O}(N^4)$ and $\mathcal{O}(N^8)$, respectively, i.e., a polynomial increase in the number of measurements [46]. As for the hardware components, we note that the tunable-coupler elements can be regarded as transmon-type qubits with a demonstrated scalability up to 20 qubits [20,22,48] and in future systems approaching 100 qubits. In such architectures, larger molecules such as water could be computed. Since the circuit depth of algorithms based on exchange-type gate is shorter than those based on CNOT gates, gate errors can be up to an order of magnitude higher to reach chemical accuracy [37].

V. CONCLUSION

In conclusion, we demonstrate a gate-efficient way to simulate molecular spectra on a tailor-made superconducting qubit processor using exchange-type two-qubit gates. With the choice of excitation-preserving exchange-type gates, tunable in both amplitude and phase, we preserve the number of excitations in the system and achieve the reduction of the VQE entangler to a single gate primitive. This enables the efficient computation of the molecular ground state, which can subsequently be used to efficiently calculate the molecule's excited states using an EOM approach. In the present case, the accuracy of the computation is still limited by the coherence time of the tunable-couple element. However, error-mitigation schemes [49,50] or minor improvements to the coherence of the coupler would allow us to reach chemical accuracy. Our findings show that adapting quantum algorithms and hardware to the problem at hand is a key requirement to perform quantum simulation on a larger scale. In particular, exchange-type gates are a promising choice to compute the energy spectra of larger molecules such as water on near-term quantum hardware.

ACKNOWLEDGMENTS

We thank the quantum team at IBM T. J. Watson Research Center, Yorktown Heights; in particular, the fab team, Jerry Chow, David McKay, and William Shanks, for insightful discussions and the provision of qubit devices. We thank R. Heller and H. Steinauer for technical support. We thank S. Hoenl for designing a teaser image for this paper. This work was supported by the IARPA LogIQ

program under Contract W911NF-16-1-0114-FE and the ARO under Contract W911NF-14-1-0124.

-
- [1] Richard P. Feynman, Simulating physics with computers, *Int. J. Theor. Phys.* **21**, 467 (1982).
- [2] Ryan Babbush, Peter J. Love, and A. Aspuru-Guzik, Adiabatic quantum simulation of quantum chemistry, *Sci. Rep.* **4**, 6603 (2014).
- [3] Alexey Yu. Kitaev, Quantum measurement and the Abelian stabilizer problem, arXiv:9511026v1.
- [4] Dave Wecker, Bela Bauer, Bryan K. Clark, Matthew B. Hastings, and Matthias Troyer, Gate-count estimates for performing quantum chemistry on small quantum computers, *Phys. Rev. A* **90**, 022305 (2014).
- [5] Austin G. Fowler, Matteo Mariantoni, John M. Martinis, and Andrew N. Cleland, Surface codes: Towards practical large-scale quantum computation, *Phys. Rev. A* **86**, 032324 (2012).
- [6] Alberto Peruzzo, Jarrod McClean, Peter Shadbolt, Man-Hong Yung, Xiao-Qi Zhou, Peter J. Love, A. Aspuru-Guzik, and Jeremy L. O'Brien, A variational eigenvalue solver on a photonic quantum processor, *Nat. Commun.* **5**, 4213 (2014).
- [7] Nikolaj Moll, Panagiotis Barkoutsos, Lev S. Bishop, Jerry M. Chow, Andrew Cross, Daniel J. Egger, Stefan Filipp, Andreas Fuhrer, Jay M. Gambetta, Marc Ganzhorn, Abhinav Kandala, Antonio Mezzacapo, Peter Müller, Walter Riess, Gian Salis, John Smolin, Ivano Tavernelli, and Kristan Temme, Quantum optimization using variational algorithms on near-term quantum devices, *Quantum Sci. Technol.* **3**, 030503 (2018).
- [8] Panagiotis K.I. Barkoutsos, Jerome F. Gonthier, Igor Sokolov, Nikolaj Moll, Gian Salis, Andreas Fuhrer, Marc Ganzhorn, Daniel J. Egger, Matthias Troyer, Antonio Mezzacapo, Stefan Filipp, and Ivano Tavernelli, Quantum algorithms for electronic structure calculations: Particle-hole Hamiltonian and optimized wave-function expansions, *Phys. Rev. A* **98**, 022322 (2018).
- [9] Ian D. Kivlichan, Jarrod McClean, Nathan Wiebe, Craig Gidney, Alan Aspuru-Guzik, Garnet Kin-Lic Chan, and Ryan Babbush, Quantum Simulation of Electronic Structure with Linear Depth and Connectivity, *Phys. Rev. Lett.* **120**, 110501 (2018).
- [10] Jarrod R. McClean, Jonathan Romero, Ryan Babbush, and Alan Aspuru-Guzik, The theory of variational hybrid quantum-classical algorithms, *New J. Phys.* **18**, 023023 (2016).
- [11] Ryan Babbush, Nathan Wiebe, Jarrod McClean, James McClain, Hartmut Neven, and Kin-Lic Garnet Chan, Low Depth Quantum Simulation of Electronic Structure, *Phys. Rev. X* **8**, 011044 (2018).
- [12] Benjamin P. Lanyon, James D. Whitfield, Geoff G. Gillett, Michael E. Goggin, Marcelo P. Almeida, Ivan Kassal, Jacob D. Biamonte, Masoud Mohseni, Ben J. Powell, Marco Barbieri, Alan Aspuru-Guzik, and Andrew G. White, Towards quantum chemistry on a quantum computer, *Nat. Chem.* **2**, 106 (2010).
- [13] Jiangfeng Du, Nanyang Xu, Xinhua Peng, Pengfei Wang, Sanfeng Wu, and Dawei Lu, NMR Implementation of a Molecular Hydrogen Quantum Simulation with Adiabatic State Preparation, *Phys. Rev. Lett.* **104**, 030502 (2010).
- [14] Bei-Bei Li, Yun-Feng Xiao, Chang-Ling Zou, Yong-Chun Liu, Xue-Feng Jiang, You-Ling Chen, Yan Li, and Qihuang Gong, Experimental observation of Fano resonance in a single whispering-gallery microresonator, *Appl. Phys. Lett.* **98**, 021116 (2011).
- [15] Chen Wang, Christopher Axline, Yvonne Gao, Teresa Brecht, Yiwen Chu, Luigi Frunzio, Michel Devoret, and Robert Schoelkopf, Surface participation and dielectric loss in superconducting qubits, *Appl. Phys. Lett.* **107**, 162601 (2015).
- [16] Christopher Monroe and Jungsang Kim, Scaling the ion trap quantum processor, *Science* **339**, 1164 (2013).
- [17] Jiehang Zhang, Guido Pagano, Paul W. Hess, Antonis Kyriianidis, Patrick Becker, Harvey Kaplan, Alexey V. Gorshkov, Z. X. Gong, and Christopher Monroe, Observation of a many-body dynamical phase transition with a 53-qubit quantum simulator, *Nature* **551**, 601 (2017).
- [18] Hannes Bernien, Sylvain Schwartz, Alexander Keesling, Harry Levine, Ahmed Omran, Hannes Pichler, Soonwon Choi, Alexander S. Zibrov, Manuel Endres, Markus Greiner, Vladan Vuletic, and Mikhail D. Lukin, Probing many-body dynamics on a 51-atom quantum simulator, *Nature* **551**, 579 (2017).
- [19] Cornelius Hempel, Christine Maier, Jonathan Romero, Jarrod McClean, Thomas Monz, Heng Shen, Petar Jurcevic, Ben P. Lanyon, Peter Love, Ryan Babbush, Alán Aspuru-Guzik, Rainer Blatt, and Christian F. Roos, Quantum Chemistry Calculations on a Trapped-Ion Quantum Simulator, *Phys. Rev. X* **8**, 031022 (2018).
- [20] Charles Neill *et al.*, A blueprint for demonstrating quantum supremacy with superconducting qubits, *Science* **360**, 195 (2018).
- [21] Johannes S. Otterbach *et al.*, Unsupervised machine learning on a hybrid quantum computer, arXiv:1712.05771.
- [22] International Business Machines Corporation, IBM Q Experience (2016).
- [23] Peter J. J. O'Malley *et al.*, Scalable Quantum Simulation of Molecular Energies, *Phys. Rev. X* **6**, 031007 (2016).
- [24] Abhinav Kandala, Antonio Mezzacapo, Kristan Temme, Maika Takita, Markus Brink, Jerry M. Chow, and Jay M. Gambetta, Hardware-efficient quantum optimizer for small molecules and quantum magnets, *Nature* **549**, 242 (2017).
- [25] James I. Colless, Vinay V. Ramasesh, Dar Dahlen, Machiel S. Blok, Jarrod R. McClean, Jonathan Carter, Wibe A. de Jong, and Irfan Siddiqi, Robust Determination of Molecular Spectra on a Quantum Processor, *Phys. Rev. X* **8**, 011021 (2018).
- [26] Pascual Jordan and Eugene Wigner, Über das Paulische Äquivalenzverbot, *Z. Phys.* **47**, 631 (1928).
- [27] Sergey B. Bravyi and Alexei Yu. Kitaev, Fermionic quantum computation, *Ann. Phys.* **298**, 210 (2002).
- [28] Felix Motzoi, Michael P. Kaicher, and Frank K. Wilhelm, Linear and Logarithmic Time Compositions of Many-Body Systems, *Phys. Rev. Lett.* **119**, 160503 (2017).
- [29] David C. McKay, Stefan Filipp, Antonio Mezzacapo, Easwar Magesan, Jerry M. Chow, and Jay M. Gambetta,

- Universal Gate for Fixed-Frequency Qubits via a Tunable Bus, *Phys. Rev. Applied* **6**, 064007 (2016).
- [30] Marco Roth, Marc Ganzhorn, Nikolaj Moll, Stefan Filipp, Gian Salis, and Sebastian Schmidt, Analysis of a parametrically driven exchange-type gate and a two-photon excitation gate between superconducting qubits, *Phys. Rev. A* **96**, 062323 (2017).
- [31] D. J. Rowe, Equations-of-motion method and the extended shell model, *Rev. Mod. Phys.* **40**, 153 (1968).
- [32] Jarrod R. McClean, Mollie E. Kimchi-Schwartz, Jonathan Carter, and Wibe A. de Jong, Hybrid quantum-classical hierarchy for mitigation of decoherence and determination of excited states, *Phys. Rev. A* **95**, 042308 (2017).
- [33] Sergey Bravyi, Jay M. Gambetta, Antonio Mezzacapo, and Kristan Temme, Tapering off qubits to simulate fermionic Hamiltonians, arXiv:1701.08213.
- [34] Andrew G. Taube and Rodney J. Bartlett, New perspectives on unitary coupled cluster theory, *Int. J. Quantum Chem.* **106**, 3393 (2006).
- [35] National Institute of Science and Technology, Computational Chemistry Comparison and Benchmark Database (2018).
- [36] John A. Pople and David L. Beveridge, *Approximate Molecular Orbital Theory* (McGraw-Hill Book Company, New York, US, 1970).
- [37] See the Supplemental Material at <http://link.aps.org/supplemental/10.1103/PhysRevApplied.11.044092> for additional information.
- [38] Sarah Sheldon, Easwar Magesan, Jerry M. Chow, and Jay M. Gambetta, Procedure for systematically tuning up crosstalk in the cross-resonance gate, *Phys. Rev. A* **93**, 060302 (2016).
- [39] Adriano Barenco, Charles H. Bennett, Richard Cleve, David P. DiVincenzo, Norman Margolus, Peter Shor, Tycho Sleator, John A. Smolin, and Harald Weinfurter, Elementary gates for quantum computation, *Phys. Rev. A* **52**, 3457 (1995).
- [40] Michael A. Nielsen and Isaac L. Chuang, *Quantum Computation and Quantum Information* (Cambridge University Press, Cambridge, UK, 2000).
- [41] Yu Chen *et al.*, Qubit Architecture with High Coherence and Fast Tunable Coupling, *Phys. Rev. Lett.* **113**, 220502 (2014).
- [42] Warren J. Hehre, Robert Ditchfield, and John A. Pople, Self-consistent molecular orbital methods. XII. Further extensions of Gaussian-type basis sets for use in molecular orbital studies of organic molecules, *J. Chem. Phys.* **56**, 2257 (1972).
- [43] Richard P. Muller, python quantum chemistry, version 2.
- [44] James C. Spall, Implementation of the simultaneous perturbation algorithm for stochastic optimization, *IEEE Trans. Aerosp. Electron. Syst.* **34**, 817 (1998).
- [45] J. Robert Johansson, Paul D. Nation, and Franco Nori, qutip2: A python framework for the dynamics of open quantum systems, *Comput. Phys. Commun.* **184**, 1234 (2013).
- [46] Pauline Ollitrault, Panagiotis Barkoutsos, Stefan Woerner, and Ivano Tavernelli, A quantum computing algorithm for the investigation of the molecular excited states (to be published).
- [47] Gadi Aleksandrowicz *et al.*, Qiskit: An open-source framework for quantum computing (2019).
- [48] Sabrina Hong, Alexander T. Papageorge, Pradaht Sivara-jah, Genya Crossman, Nicolas Didier, Anthony Polloreno, Eyob A. Sete, Stefan W. Turkoswki, Blake R. da Silva, and Marcus P. Johnson, Demonstration of a parametrically-activated entangling gate protected from flux noise, arXiv:1901.08035.
- [49] Kristan Temme, Sergey Bravyi, and Jay M. Gambetta, Error Mitigation for Short Depth Quantum Circuits, *Phys. Rev. Lett.* **119**, 180509 (2017).
- [50] Abhinav Kandala, Kristan Temme, Antonio D. Corcoles, Antonio Mezzacapo, Jerry M. Chow, and Jay M. Gambetta, Extending the computational reach of a noisy superconducting quantum processor, arxiv:1805.04492.